Muon $g-2$ at a multi-TeV muon collider

Wen Yin[1,2] and Masahiro Yamaguchi[2]
[1]Department of Physics, University of Tokyo, Tokyo 113-0033, Japan
and Department of Physics, KAIST, Daejeon 34141, Korea
[2]Department of Physics, Tohoku University, Sendai, Miyagi 980-8578, Japan

(Received 30 December 2020; accepted 18 August 2022; published 30 August 2022)

The long-standing discrepancy of the muon anomalous magnetic moment $(g-2)$ is a hint of new physics beyond the standard model of particle physics. In this paper, we show that heavy new physics contribution can be fully tested at a muon collider with a center-of-mass energy up to $\mathcal{O}(10)$ TeV with $\mathcal{O}(10)$ ab^{-1}. Even if there is no new particle in this energy range, one can measure the $g-2$ operator directly via the channel to a Higgs boson and a monochromatic photon. In particular, the latter process, which is the most challenging case, can be tested in the $20[50]\times(\frac{L_i}{40\ \text{ab}^{-1}})^{-1/2}$ TeV muon collider at the 2 [5] σ level with L_i being the integrated luminosity if the efficiency of the detector built in the future is almost perfect.

DOI: 10.1103/PhysRevD.106.033007

I. INTRODUCTION

The long-standing discrepancy of the muon anomalous magnetic moment $(g-2)$ is the leading candidate suggesting new physics beyond the standard model (BSM) that couples to the standard model (SM) particles. The muon $g-2$ anomaly indicates the more than 3 σ level deviation of

$$\Delta a_\mu = a_\mu^{\text{EXP}} - a_\mu^{\text{SM}} = (27.4 \pm 7.3)\times 10^{-10}, \qquad (1)$$

where a_μ^{SM} is the SM prediction of the muon $g-2$ from the so-called R-ratio approach [1,2] and a_μ^{EXP} is its experimental result [3,4]. (see also [5–7]) The ongoing experiment E989 at Fermilab [8] and the upcoming one at J-PARC [9] may significantly increase the accuracy of the experimental value. On the other hand, the leading order vacuum polarization contribution was recently calculated by Borsanyi *et al.* in the lattice QCD [10] and was argued to resolve the tension, although the result is still in debate [11,12]. Therefore, in order to confirm the discrepancy, efforts are being made on both experimental and theoretical sides. For instance, the MUonE experiment was proposed to perform a competitive and independent determination of the hadronic vacuum polarization (see Ref. [13] and the references therein). In this paper, on the contrary, we propose a high energy test of the $g-2$. This is not bothered by the QCD nonperturbative effect.

On the model-building side, if an ultraviolet (UV) theory generates the $g-2$ anomaly, the resulting low energy effective theory should have the muon $g-2$ operator given by

$$\Delta\mathcal{L}_{\text{eff}} \supset \frac{e\Delta\alpha_\mu}{4m_\mu}\bar{\mu}\sigma_{\mu\nu}F^{\mu\nu}\mu. \qquad (2)$$

Here, $m_\mu \simeq 0.11$ GeV is the muon mass, where $\sigma_{\mu\nu}\equiv i[\gamma_\mu,\gamma_\nu]/2$, and $F^{\mu\nu}$ is the field strength of photon. In this UV explanation, we may either have new states much heavier than m_μ to generate (2) or have a strongly coupled theory at the high energy since (2) is a higher dimensional term. On the contrary, the $g-2$ may be also explained due to a weakly coupled light particle, below or around the muon mass, i.e., an infrared (IR) explanation.

In this paper, we point out that the UV explanation scenarios can be fully tested at a muon collider [14–16] (see also recent studies for BSM [17–20]) with a center-of-mass energy, E_{cm}, up to $\mathcal{O}(10)$ TeV. This is because the heavy new physics relevant to the discrepancy must couple to the muon and thus, should leave traces in muon-antimuon collisions. The new particles in the reachable energy scales can be produced in the collider by the diagram cutting the propagator in the $g-2$ loop, and thus, the $g-2$ can be tested (see Fig. 1). In particular, if the heavier BSM particle in the loop is produced, it must decay according to the cutting of the $g-2$ diagram. If the BSM particles are so heavy that they are not reachable, or if there exist just various higher dimensional operators

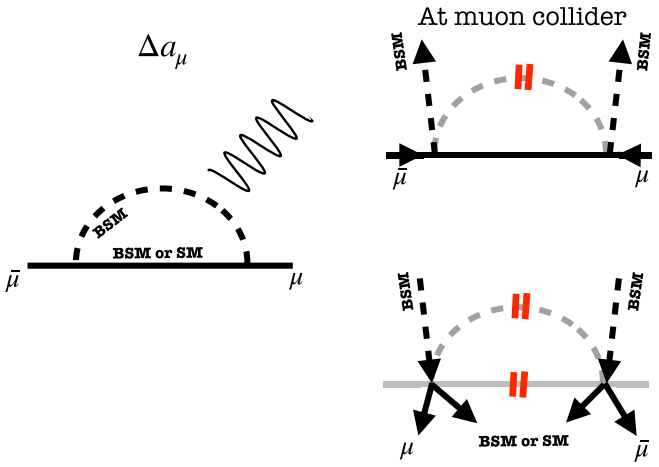

FIG. 1. A general approach to test the muon $g-2$ in the muon collider when the BSM particle masses are within reach of a muon collider. The heavy BSM particle in the loop of the muon $g-2$ becomes on shell at the collider via the coupling relevant to the $g-2$. The BSM particle decays from the diagram by cutting both propagators if the kinematics allows.

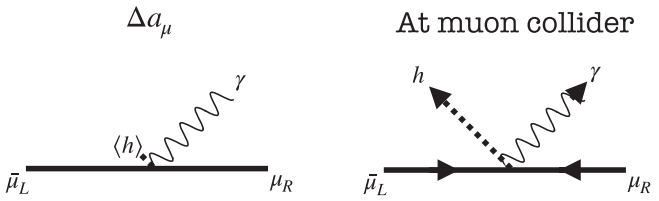

FIG. 2. The general effective theory approach for the collider test of the muon $g-2$. When the BSM particles are much heavier than the collider reach, the operator can be directly measured via $\mu\bar{\mu} \to h\gamma$ process.

without new particles, the process $\mu\bar{\mu} \to h\gamma$, where h is a Higgs boson and γ is a monochromatic photon, via a dimension six operator is a robust prediction (see Fig. 2). This process has a suppressed SM background. Consequently, the new physics contribution to the muon $g-2$ can be measured at the muon collider by measuring this cross section.

A muon collider test of the $g-2$ was studied by the authors of Ref. [21], by focusing on the lightest new particle, which is assumed to be reachable at the muon collider. In this paper, we will show that even if none of the new particles is reachable, the muon $g-2$ can be tested. In the reachable case, on the other hand, we provide complementary approaches, e.g., measuring the charged decay products of a heavier new particle. This should be the simplest way, in certain cases, e.g., if the lightest one does not have a charge, and the heavier one is reachable. Also, from the properties of the produced new particles, we may "measure" the $g-2$ by calculating the corresponding loop contribution.

II. MUON $g-2$ FROM GEV–TEV PHYSICS AND MUON COLLIDER

Let us consider a general renormalizable UV theory. The $g-2$ operator (2) can be generated through loop diagrams including new states. At the 1-loop level,[1] the diagram can be composed of the following set of particles:

$$(X_1, P_i^{\rm SM}) \quad \text{or} \quad (X_1, X_2), \tag{3}$$

where X_i and $P_i^{\rm SM}$ denotes BSM particles and SM particles, respectively. The sum of the electromagnetic charges of the two particles is -1, which is the charge of the muon.

In either case, the BSM particles in the loop can be produced in the muon collider by cutting the propagator. In the left panel of Fig. 1, we display the general 1-loop diagram for the $g-2$, including both cases. In the right panel, we show the collider production of the BSM particles in the loop. If the heavier particle in the loop is produced, it must decay, corresponding to the cutting of both propagators. By detecting the BSM particle or its decay, we can test the $g-2$.

A. A general approach in renormalizable theory

Before discussing a detailed model, let us make a general discussion. To test the former case, one may generally measure the cross section of the SM process, $\mu\bar{\mu} \to P_i^{\rm SM}\bar{P}_i^{\rm SM}$, which is from a X_1 mediated diagram (See Appendix B). (If $P_i^{\rm SM}$ is a neutrino, the discussion would be almost the same as the second case.) In the context of $X_1 = Z'$ or neutral BSM particle, it was shown in Refs. [21,22] a significant enhancement of the scattering cross section of $\mu\bar{\mu} \to \mu\bar{\mu}$ can be made and that the muon collider should be possible to discriminate the scenario from the SM. This is the case that Z' is heavy enough. In fact, a light Z' can also explain the muon $g-2$ anomaly with a small coupling, which is an IR scenario and is not our focus (see, on the other hand, the Z' search in DUNE, M^3, and NA64 [23–25]).

In both cases, on the other hand, we can cut the propagator of a BSM particle in the loop in Fig. 1. If the center-of-mass scale is higher than the BSM scale, this becomes the diagram for the production of the BSM particle at the muon collider as the right top diagram in Fig. 1. In the remainder of this subsection, we use the notation of the latter case in Eq. (3), but our discussion holds for the former case by replacing X_1 to be X and X_2 to be $P_i^{\rm SM}$. Suppose that the typical coupling among the muon (s) and the new particle(s) is g and the heaviest new particle

[1]At a higher loop, the production cross section at the muon collider should be even enhanced, and the scenario is easier to be tested. The tree-level process is not important in renormalizable UV theory.

in the loop is X_1, whose mass is M_X. The muon $g-2$ contribution can be denoted in the form,

$$\delta\alpha_\mu = \kappa \frac{m_\mu^2 g^2}{16\pi^2 M_X^2}, \tag{4}$$

where κ is a model-dependent function of parameters. κ can be either $\mathcal{O}(1)$ or larger than 1. This notation follows the SUSY models [26–29]. We will show an upper limit of κ in a particular model from phenomenology. As one can see from the left diagram in Fig. 1, g^2 can be regarded as the product of two couplings $g^2 = |g_1 g_2|$ in Eq. (4) with g_1 and g_2 being the couplings for the two vertices (the photon vertex has the coupling, $\sim e$, in the renormalizable model; see c.f. Appendix B for a nonrenormalizable case). This is the case in various models (see, e.g., Sec. II 2). We can define the typical coupling g because the $|g_1 g_2|$ will be required to be not very small in the UV explanation of the muon $g-2$. In addition, $|g_1|, |g_2| < \mathcal{O}(1)$ from the perturbativity, and thus, we cannot have a large hierarchy between $|g_1|$ and $|g_2|$. This allows us to have $|g_1| \sim |g_2| \sim g$. In addition, as we will see in Sec. II 2, a difference between $|g_1|$ and $|g_2|$ will make the model easier to be tested.

To explain the discrepancy,

$$M_X = 340\ \text{GeV} \times g\sqrt{\kappa}\sqrt{\frac{2.7\times 10^{-9}}{\delta\alpha_\mu}}. \tag{5}$$

Therefore, even if $g\sqrt{\kappa} = \sqrt{4\pi}$, which is around the perturbative unitarity bound with $\kappa \sim \mathcal{O}(1)$, the mass of the new state is around 1 TeV and thus, is reachable in the muon collider with the center-of-mass energy $\mathcal{O}(1\text{–}10)$ TeV. On the other hand, if $\kappa \gg 1$ and $g = \mathcal{O}(1)$, M_X may be much heavier than TeV beyond the reach of the collider. The former will be discussed in this section, while the last case will be tested by the proposal in the next section.

The question is whether the heavy state can be significantly produced. In fact, by cutting the heavy state propagator in the loop for the muon $g-2$, one gets a $\mu + \bar{\mu} \to X_1 + \bar{X}_1$ process. The corresponding cross section can be estimated as

$$\simeq \kappa_2 \frac{g^4}{4\pi E_{\text{cm}}^2} \quad (\text{for } E_{\text{cm}} > 2M_X). \tag{6}$$

Here, κ_2 is another model-dependent function of momentum and parameters, and E_{cm} is the center-of-mass energy. $\kappa_2 = \mathcal{O}(1)$ if there is no suppression, e.g., chirality suppression, in the production process.

By using (5) and eliminating g in (6), the lower bound of the cross section can be obtained as

$$\sigma \gtrsim 6\ \text{pb} \times \frac{\kappa_2}{\kappa^2}\left(\frac{M_X}{250\ \text{GeV}}\right)^4 \left(\frac{20\ \text{TeV}}{E_{\text{cm}}}\right)^2 \left(\frac{\delta\alpha_\mu}{2.7\times 10^{-9}}\right). \tag{7}$$

Here, we take the inequality because there could be other processes like a Drell-Yan production of $X_1, \bar{X}_1$ pair if X_1 is charged. The production via the diagram in Fig. 1 is a t-channel process, while the Drell-Yan production is an s-channel one. Thus, they typically have different angular distributions of the produced particles.

The cross section (6) is suppressed if $\kappa \gg 1$ and $g \ll 1$. Even in this case, $\frac{\kappa_2}{\kappa^2} \gtrsim \frac{m_\mu^2}{M_X^2}$ should be satisfied because the production involving the chirality flipping diagram is also enhanced according to the cut (see Fig. 1). That said, it is difficult to find a realistic model with $g \to 0, \kappa \to \infty$ to explain the muon $g-2$ (see Sec. II 2).

The number of events for $X_1, \bar{X}_1$ pair production is

$$N \simeq 4\times 10^7 \left(\frac{\sigma}{1\ \text{pb}}\right)\left(\frac{L_i}{40\ \text{ab}^{-1}}\right). \tag{8}$$

We remind that L_i is the integrated luminosity. If X_1 does not carry any charge, X_1 soon decays to a muon and a charged new particle. This process should be searched for analog to the dilepton search in the context of Z' [30,31]. If X_1 is charged, on the other hand, it may decay into a muon and a neutral state. Thus, the event should be

$$\mu + \bar{\mu} \to X_1 + \bar{X}_1 \to \mu + \bar{\mu} + X_2 + \bar{X}_2,$$

where X_2 is assumed to be lighter than X_1. The dominant background, e.g., if X_2 is neutral, is [20] $\mu + \bar{\mu} \to$ vector bosons $\to \mu + \bar{\mu} + \nu_\mu + \bar{\nu}_\mu$. Notice that in the muon collider, the center-of-mass colliding energy is given, unlike the hadron collider. Thus, one can study the kinematics of the out-going muons to identify the masses of the new particles, e.g., for the background case, two outgoing muons are almost back to back. This is in contrast with the new physics case: since X_1 is massive, the produced muons are not so back to back. In any case, the acoplanar dileptons in excess of expectations of WW and ZZ production are the signal a la slepton searches in lepton colliders [32,33]. (For comparison, the SM cross section of $\mu\bar{\mu} \to \mu\bar{\mu} +$ missing is below a few fb with the center-of-mass energy $\sim$10 TeV [20].) On the other hand, we may also have more exotic decay products if X_1 dominantly couples to them. Then they are easier to detect than the neutral particles above and thus can certainly be detected.

It is noteworthy to mention that one may measure the masses and spins of X_1, and X_2, and the renormalizable couplings to muon via the production cross sections, and thus, one may reconstruct the $g-2$ diagram (see Appendix for the model of Sec. II 2). A more detailed study on measuring the BSM couplings will be discussed elsewhere.

B. Testing muon $g-2$ in a muon-smuon-bino like system

In this part, we discuss the latter case of (3) in a concrete model. Let us consider

$$\mathcal{L}_{\rm int} = -g_1 \bar{\mu}_L \hat{P}_L \phi_R \lambda - g_2 \bar{\mu}_R \hat{P}_R \phi_L \lambda + \delta M^2 \phi_L^* \phi_R + \text{H.c.}, \tag{9}$$

where λ is a Majorana fermion with mass term $\mathcal{L}_\lambda = \frac{M_\lambda}{2}\lambda^c\lambda$ while $\phi_{L,R}$ are complex scalars with mass terms $\mathcal{L}_{L,R} = -m_L^2|\phi_L|^2 - m_R^2|\phi_R|^2$; μ_L and μ_R represent the left- and right-handed muon, respectively. This Lagrangian with restricted parameter relations can be identified as the one from the minimal supersymmetric SM (MSSM), in which λ and $\phi_{L,R}$ are identified as bino and smuons, respectively. In the MSSM, $\delta M^2 = -m_\mu(\mu\tan\beta - A_\mu)v$, $g_1 = -\sqrt{2}g_Y$, $g_2 = 1/\sqrt{2}g_Y$, by neglecting the radiative corrections with g_Y being the coupling of the $\mathrm{U}(1)_Y$ symmetry, and $v \simeq 174$ GeV is the vacuum expectation value (vev) of the Higgs field, h, but we do not force this relation.[2]

The muon $g-2$ contribution is calculated as (c.f. Ref. [38])

$$\delta a_\mu \simeq -\frac{g_1 g_2}{16\pi^2}\frac{m_\mu \delta M^2 M_\lambda}{m_L^2 m_R^2} f\left(\frac{m_L^2}{M_\lambda^2}, \frac{m_R^2}{M_\lambda^2}\right), \tag{10}$$

where we have used the mass insertion approximation on the scalar mixings of δM^2 and $f(x,y) = xy\left(\frac{-3+x+y+xy}{(x-1)^2(y-1)^2} + \frac{2x\log x}{(x-y)(x-1)^3} - \frac{2y\log y}{(x-y)(y-1)^3}\right)$. This satisfies $0 < f(x,y) < 1$ and $f(1,1) = 1/6$. δM^2 should satisfy

$$\delta M^2 \lesssim \min\left[m_L^2, m_R^2\right]. \tag{11}$$

Otherwise, not only our approximation of mass insertion in (10) is invalid, but also there are dangerous tachyonic scalars or vacuum instability (c.f. Ref. [39]). Strictly speaking, the vacuum stability requires a more stringent bound of $\frac{\delta M^2}{v} \lesssim \min\left[m_L, m_R\right]$. This makes the model easier to be tested.

Let us check the minimal production cross section of the new particles at the muon collider. By fixing g_1, g_2, $\delta\alpha_\mu$ becomes the largest when $M_\lambda \sim m_L \sim m_R \sim \sqrt{|\delta M^2|}$. With the relation, we obtain the maximum contribution as

$$|\delta a_\mu| \lesssim \frac{|g_1 g_2|}{16\pi^2}\frac{m_\mu}{M_\lambda} f \simeq 2\times 10^{-9}\left(\frac{|g_1 g_2|}{0.02}\right)\left(\frac{1\ \text{TeV}}{M_\lambda}\right)^2\left(\frac{f}{1/6}\right). \tag{12}$$

As mentioned previously, $|g_1| \gg |g_2|$ or $|g_1| \ll |g_2|$ is difficult to have. This is because the BSM particle scales are around or higher than TeV, and $|g_1 g_2|$ has a lower bound while $\max[|g_1|, |g_2|] > \sqrt{|g_1 g_2|}$ has an upper bound of $\mathcal{O}(1)$ from the perturbativity. This justifies the use of the typical coupling g in the previous general discussion. More precisely, the production cross section to ϕ_L, ϕ_R, or λ pair through the new couplings are

$$\sigma^{g_{1,2}}_{\mu\bar{\mu}\to\phi_L\phi_L^*,\phi_R\phi_R^*} \sim \frac{g_{1,2}^4}{128\pi E_{\rm cm}^2} \times (\log(4/\epsilon^2) - 2),$$
$$\sigma^{g_{1,2}}_{\mu\bar{\mu}\to\lambda\bar{\lambda}} \sim \frac{g_1^4 + g_2^4}{32\pi E_{\rm cm}^2}. \tag{13}$$

Here, ϵ is the IR cutoff of our calculation by neglecting the mass, e.g., $\epsilon \sim |M_\lambda|/E_{\rm cm}$ for $|M_\lambda| \sim m_L \sim m_R$. The cross section of $\mu\bar{\mu} \to \phi_L\phi_R^*$ or $\mu\bar{\mu} \to \phi_R\phi_L^*$ is further suppressed by $(\delta M^2/(m_L^2 - m_R^2))^2$ or $M_\lambda^2/E_{\rm cm}^2$. Thus, the sum of the cross sections are minimized at $|g_1| = |g_2|$ with fixing the product $|g_1 g_2|$ and the dimensionful parameters. This means that the BSM particles are more frequently produced with $|g_1| \neq |g_2|$.

In addition, there is also the usual Drell-Yan production of ϕ_L pair or ϕ_R pair. This s-channel cross section mediated by an off shell photon is given as

$$\sigma^{\text{Drell-Yan}}_{\mu\bar{\mu}\to\phi_L\phi_L^*,\phi_R\phi_R^*} \sim \frac{e^4}{24\pi E_{\rm cm}^2} \sim 0.1\ \text{fb}\left(\frac{20\ \text{TeV}}{E_{\rm cm}}\right)^2. \tag{14}$$

By taking into account the Z-boson contribution, the cross section can differ by an $\mathcal{O}(1)$ factor.

From Eq. (12), the smaller of $|g_1|$ and $|g_2|$ is larger than e when $|M_\lambda|$ is higher than TeV. Therefore, the cross section in Eq. (13) can be larger than Eq. (14) when the BSM scales are higher than TeV. Since the "sleptons" can be produced with $L_i = 40\ \text{ab}^{-1}$ with $E_{\rm cm} = 20$ TeV, they can be easily detected due to the clean environment like the case of electron-positron collider (e.g., [32,33,39]). Also, when $\lambda\bar{\lambda}$ are produced, one can search for its decay product as discussed previously.

So far, we have assumed that the new states relevant to the muon $g-2$ are all reachable at the muon collider. We have discussed various processes relevant to the BSM particles by noticing that the two kinds of loop components in Eq. (3) must include a charged particle. Then from the detection of the charged BSM particle or measurement of

[2]In the context of MSSM, the so-called Higgs mediation mechanism [26], which is proposed by the present authors, can lead to the sizable contribution to the muon $g-2$ with this effective Lagrangian. For scenarios involving the Higgs mediation in explaining the muon $g-2$ anomaly, see Refs. [26–29,34], and explaining both muon and electron $g-2$ anomaly [35,36]. Also see Ref. [37] for the $E_7/\mathrm{SU}(5)\times\mathrm{U}(1)^3$ unification of family. In the scenario, the mass degeneracy between bino and wino is "predicted" to be within $\mathcal{O}(1)\%$. Thanks to the Higgs mediation, the bino can be the dominant dark matter with a bino-wino coannihilation, and, moreover, the bottom-tau Yukawa coupling unification can be achieved up to $\mathcal{O}(1)\%$.

the kinematics of the final leptonic charged states, the muon collider can probe the $g-2$. The production cross sections of the BSM particles are larger than $\mathcal{O}(\mathrm{fb}-\mathrm{pb})$, which implies a number of events more than $\mathcal{O}(10^{3\text{–}6})$. By assuming that the detector sensitivity is ~ 1 and no significant background in this future lepton collider for the new resonance or the leptonic kinematics c.f. [40,41], we can conclude that the muon $g-2$ can be tested in this case.

A generic concern is that charged or all of the BSM particles may be heavier than the reach of the collider. We discuss the former case in Appendix B from the topology and the muon chirality flip of the Feynman diagrams in singlets extension of the SM effective theory. We show that the maximal cutoff scale in the effective theory is $\lesssim 10$ TeV, which implies that we probably do not have this possibility. In addition, even if the effective theory is valid, and even if the singlets dominantly decay into missing energy, the whole singlet extended possibilities are fully tested in the muon collider.

The most difficult situation is that all the BSM particles are out of reach. Alternatively, there may be no new particle with only higher-dimensional operators. Then the direct production of particles is difficult/impossible at the muon collider with $\mathcal{O}(10)$ TeV. Nevertheless, in the next section, we show that the muon $g-2$ can be directly tested by measuring $\mu\bar{\mu} \to h\gamma$.

III. MEASURING MUON $g-2$ IN EFFECTIVE THEORY

Now let us assume the possibility that no new physics state is reachable at the muon collider. The $g-2$ operator is directly related with the coupling to the Higgs boson, h, as

$$\Delta\mathcal{L}_{\mathrm{eff}} \supset \frac{y_\mu}{M^2}\frac{h}{\sqrt{2}}\bar{\mu}\sigma_{\mu\nu}F^{\mu\nu}\mu, \tag{15}$$

where we have used $m_\mu = y_\mu v$ and have replaced v to be $v + h/\sqrt{2}$ from Eq. (2), and y_μ/M^2 is the dimension -2 coupling. In the symmetric phase, we may also have a vertex of muons, Higgs field, and Z (W) boson, which will increase detection channels. However, the embeddings of the $g-2$ operator in the electroweak symmetric terms are model dependent, and we do not consider them. One may also consider dimension > 6 terms to generate (2) with several Higgs fields. In this case, still, we get a similar dimension 6 term with several Higgs fields replaced by the VEV, and the cross section of $\mu\bar{\mu} \to h\gamma$ can be enhanced by $\mathcal{O}(1\text{–}10)$ from what we will show. A possible loophole relevant to the generic higher dimensional term is the cancellation among the higher dimensional terms. This will be discussed in the next section, and we will show that the multi-Higgs/gauge boson plus γ emission can be tested. Since, in a natural setup, the contribution from the dimension 6 terms should be dominant, we focus on the single operator Eq. (15) in this section.

Here, to explain the anomaly (1),

$$M \simeq 7.6\ \mathrm{TeV}\left(\frac{2.7\times 10^{-9}}{\Delta\alpha_\mu}\right)^{1/2}. \tag{16}$$

Notice that (15) is a dimension-six term, which becomes stronger in the collisions of muon-antimuon at higher energy.[3]

The robust prediction of the muon $g-2$ anomaly in the effective theory is the enhancement on h and γ production of

$$\mu + \bar{\mu} \to h + \gamma, \tag{18}$$

at high energy. This provides a signal of a monochromatic photon with energy $\sim E_{\mathrm{cm}}/2$ and two fermions or four fermions with the invariant mass of the Higgs boson. The production cross section of $h\gamma$ can be calculated as

$$\sigma^{g-2}_{\mu\mu\to\gamma h} \simeq \frac{y_\mu^2 E_{\mathrm{cm}}^2}{48\pi M^4} \sim 0.1\ \mathrm{ab}\left(\frac{E_{\mathrm{cm}}}{20\ \mathrm{TeV}}\right)^2\left(\frac{7.6\ \mathrm{TeV}}{M}\right)^4, \tag{19}$$

where we have neglected the masses of the initial and final states. Here, we have used y_μ at the renormalization scale $\mu_{\mathrm{RG}} \sim m_\mu$. For a more precise value, one may use the muon Yukawa coupling at $\mu_{\mathrm{RG}} \sim E_{\mathrm{cm}}$ to take into account a dominant part of the renormalization group running of (15).

The cross section at the tree level is plotted in Fig. 3. The process $\mu + \bar{\mu} \to h + \gamma$ is absent in the SM at the tree level with neglecting the muon mass. At the loop level, for instance, the top-loop-induced contribution is

$$\sigma^{\mathrm{SM}}_{\mu\mu\to\gamma h} \sim \frac{y_t^2 e^6}{(4\pi)^5}\frac{1}{E_{\mathrm{cm}}^2} = 0.002\ \mathrm{ab}\left(\frac{20\ \mathrm{TeV}}{E_{\mathrm{cm}}}\right)^2. \tag{20}$$

Thus, this can be safely neglected at a multi-TeV muon collider. The background of $\mu\bar{\mu} \to Z\gamma$ or $\mu\bar{\mu} \to W^+W^-\gamma$ is suppressed with multi-TeV of E_{cm},[4] since the cross section decreases with larger E_{cm} and since they have different chiralities of initial muons (c.f. Refs. [42–44]).

[3]The scale that effective field theory is valid can be much higher than the reach of the muon collider. This is because M in our notation corresponds to

$$M_* \simeq 310\ \mathrm{TeV}\frac{M}{7.6\ \mathrm{TeV}}, \tag{17}$$

of the higher dimensional term $\frac{h}{\sqrt{2}M_*^2}\bar{\mu}\sigma_{\mu\nu}F^{\mu\nu}\mu$.

[4]In principle, we can also test the $\mu\bar{\mu} \to h\gamma$ process in renormalizable UV models for the muon $g-2$. In this case, the cross section is smaller at higher E_{cm} if the new particle masses are much smaller than E_{cm} and the background process may be dominant. It may be important to polarize the muons. This may be possible since they are produced from pion decays.

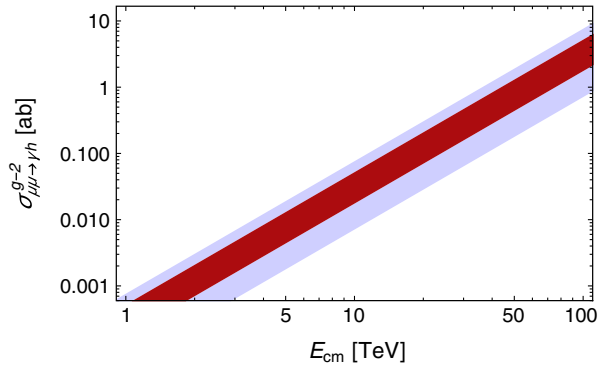

FIG. 3. The cross section of $\mu\bar{\mu} \to h\gamma$ via the muon $g-2$ operator (15) by varying the center-of-mass energy. The red (blue) band corresponds to the 1σ (2σ) region of the muon $g-2$ anomaly.

In this case, the cross section (19) is not as large as the previous section's ones. To check whether the muon collider can provide a test, let us define the signal significance by

$$\frac{N_S}{\sqrt{N_S + N_B}}, \tag{21}$$

where $N_S = R_{\rm det} \times N$ is the number of events that are detected with $R_{\rm det}$ being the detector sensitivity. $N \sim 4(\frac{L_i}{40\ {\rm ab}^{-1}})(\frac{\sigma^{g-2}_{\mu\bar{\mu}\to\gamma h}}{0.1\ {\rm ab}})$ is the number of events that can happen in the collider, and N_B is the detected number of background events. For a 5 [2] σ excess of the events from the SM background by taking $N_B \sim 0$, we need at least 25 [4] events to be detected. The 5σ [2σ] significance is achieved if we build a $50[20] \times (\frac{L_i}{40\ {\rm ab}^{-1}})^{-1/2}$ TeV muon collider if the detector efficiency is perfect, $R_{\rm det} \sim 1$.

The designs of the detectors of the muon collider are not determined, and there are still several challenges. In particular, the muon in the beam decays to $e\nu\bar{\nu}$ [15],[5] and the electron may radiate a photon. This photon, together with a vector-fusion Higgs boson, may contribute to the background of $\mu\bar{\mu} \to h\gamma$. Such a photon should be difficult to carry the momentum around half of the center-of-mass energy, and thus, we consider it irrelevant. Alternatively, the specific environment might pay the price of the detector sensitivity. The detector effects depend on the future environment of the muon collider. To clarify them is beyond our scope. In any case, as long as $R_{\rm det} = 0.1$–1, and $N_B \lesssim N_S$, we can exclude the $g-2$ operator at the 2σ level at $\mathcal{O}(10)$ TeV, $\mathcal{O}(10)$ ab^{-1} muon collider.

[5]It may be also interesting to use the neutrino to probe the muon $g-2$ via, e.g., $\mu^-\bar{\nu}_\mu \to \gamma W^-$ from the same operator via the equivalence theorem for the W^- and the charged would-be Nambu-Goldstone boson.

In this section, we have discussed the most difficult case for probing the $g-2$ at the muon collider, and we have found that it is viable. As a consequence, the muon $g-2$ can be tested at the 20 TeV (50 TeV) muon collider at $2\sigma(5\sigma)$ level with 40 ab^{-1} luminosity if the detector efficiency is perfectly good.

IV. PROBING MUON $g-2$ WITH UNNATURAL EFTS

So far, we pointed out that even if the BSM particles are not reachable in the muon collider, the $g-2$ can be tested via $\mu\bar{\mu} \to h\gamma$ in the EFT with the operator (15). We implicitly assumed that there are no other terms that cancel the amplitude of the process. In this section, we discuss some unnatural EFTs that might hide the channel of $\mu\bar{\mu} \to h\gamma$. We will show, even in this case, that the $\mathcal{O}(10)$ TeV muon collider can test the $g-2$.[6]

Before discussing this in more detail, let us mention that there are bounds for the largest center-of-mass energy from the perturbative unitarity or the cutoff of the EFT. In particular, when the center-of-mass energy is too large, the EFT approach should not be applicable, while the criterion on the scale depends on the underlying theory. In this section, we will not take the bound as a guiding principle.

A. Generic SMEFT with cancellation of the Higgs coupling

For concreteness and simplicity, let us consider the following EFT coupling of the muon $g-2$ operator,

$$\mathcal{L}_{\rm EFT} \supset -F(H_0)\bar{\mu}\sigma_{\mu\nu}F^{\mu\nu}\mu. \tag{22}$$

Here, $H_0 = v + h/\sqrt{2}$ is the CP-even neutral component of the Higgs doublet. We neglect to write down the electroweak partners of the neutral CP-even Higgs field and the photon for the model-independent discussion. We emphasize again that the gauge invariance should be guaranteed when we recover the partners. Let us consider

$$F(H_0) = \sum_{i=0}^{N_{\rm max}} \frac{c_i}{v^{2+2i}(2i+1)!} H_0^{2i+1}, \tag{23}$$

where c_i are the dimensionless coefficients, and $N_{\rm max}$ corresponds to the dimension of the highest dimensional operator, $d_{\rm max} = (2N_{\rm max} + 6)$. We set a finite $N_{\rm max}$ for the convenience of analysis. We will check that our conclusions do not change by varying $N_{\rm max}$. In general, we also have terms, e.g., with derivatives and other fields. We will discuss them in the last of this part.

[6]We thank the two referees for suggesting we study the loopholes in this section.

To explain the muon $g-2$ anomaly, we have

$$F(v)=\sum_{i=0}^{N_{\max}}\frac{c_i}{v(2i+1)!}=\frac{e\Delta\alpha_\mu}{4m_\mu}. \tag{24}$$

With $N_{\max}>0$, we have various operators with nonvanishing c_i to satisfy Eq. (24). They may all contribute to $\mu\bar{\mu}\to h\gamma$. Thus, there may be a certain cancellation between the amplitudes of $h\gamma$ production from different terms in Eq. (23), although it is unnatural.

To study the possibility, let us check the cross section of $\mu\bar{\mu}\to\gamma nh$. This can be approximated as

$$\sigma_{\mu\bar{\mu}\to\gamma nh}\sim\left|\frac{F^{(n)}(v)}{2^{n/2}}\right|^2\frac{E_{\rm cm}^{2n}}{(4\pi)^{2n-1}n!}, \tag{25}$$

where the power of $E_{\rm cm}$ is from the dimensional argument, and the denominator is for the phase space [remind that the cross section corresponds to the imaginary part of an n-loop diagram, and $n!$ reflects the n identical (Higgs) bosons in the final state]. We also defined $F^{(n)}(X)\equiv\frac{\partial^n}{\partial X^n}F(X)$. The cancellation of the $\bar{\mu}\mu\to nh\gamma$ happens if $F^{(n)}(v)\approx 0$ and $c_i\neq 0$ with $i\geq(n-1)/2$. We note that in this setup, the cancellation does not depend much on the center-of-mass scale since $F^{(n)}(v)$ does not depend on the center-of-mass scale. Thus, it may be difficult to remove this cancellation with experiments with several different $E_{\rm cm}$.[7] On the other hand, we cannot cancel the amplitude or the cross section for all n. This is because we cannot satisfy both Eq. (24) and $F^{(n)}(v)=0$ for all $n\geq 1$.

To take account of the cancellation, we estimate the "inclusive" $g-2$ cross section,

$$\sigma_{\rm tot}^{g-2}[E_{\rm cm},N_{\max}]\equiv\sum_{n=1}^{2N_{\max}+1}\sigma_{\mu\bar{\mu}\to\gamma nh}. \tag{26}$$

We can estimate the lowest value of the inclusive cross section via the BSM process,

$$\min_{c_i}\sigma_{\rm tot}^{g-2}[E_{\rm cm},N_{\max}], \tag{27}$$

for fixed $N_{\max}$, $E_{\rm cm}$ and Eq. (24) by varying c_i. The results are shown in Fig. 4 in the $N_{\max}-\frac{\min_{c_i}\sigma_{\rm tot}^{g-2}[N_{\max},E_{\rm cm}]}{\sigma_{\rm tot}^{g-2}[1,E_{\rm cm}]}$ plane with $E_{\rm cm}=50$ TeV (the upper red circles) and

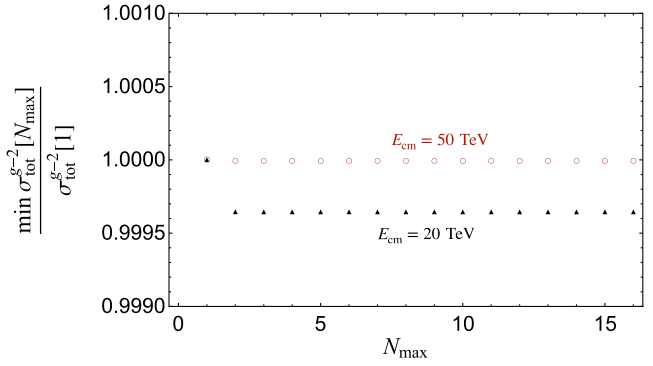

FIG. 4. $N_{\max}$ vs $\frac{\min\sigma_{\rm tot}^{g-2}[N_{\max},E_{\rm cm}]}{\sigma_{\rm tot}^{g-2}[1,E_{\rm cm}]}$. The red circle (black triangle) corresponds to $E_{\rm cm}=50$ TeV (20 TeV).

$E_{\rm cm}=20$ TeV (the lower black triangles).[8] This result means that including higher dimensional terms to cancel $\mu\bar{\mu}\to nh\gamma$ process with smaller n leads to a larger inclusive cross section due to the process with a larger n. Thus, the smallest cross section turns out to be $c_{i\neq 0}\approx 0$, $c_0\approx\frac{ve\Delta\alpha_\mu}{4m_\mu}$.

To understand the behavior, let us focus on a simple example with $N_{\max}=1$. We can easily find that we have the cancellation of the amplitude of the $n=1$ process, $\bar{\mu}\mu\to h\gamma$, only if $c_0=\frac{3}{2}\frac{ve\Delta\alpha_\mu}{4m_\mu}$, $c_1=-3\frac{ve\Delta\alpha_\mu}{4m_\mu}$. This leads to the higher dimensional scale, $(v^{2+2i}(2i+1)!/c_i)^{1/(2i+2)}\sim v(ve\Delta\alpha/m_\mu)^{-1/(2i+2)}$. The $i=1$ case has a much lower scale than $i=0$ case. Therefore, the $\mu\bar{\mu}\to 2h\gamma, 3h\gamma$ will be highly enhanced at large $E_{\rm cm}$. In fact, the minimal inclusive cross section is obtained by minimizing $\sigma_{\rm tot}^{g-2}\sim(c_0+c_1/2)^2\frac{(E_{\rm cm})^2}{(8\pi v^4)}+(c_1)^2\frac{(E_{\rm cm})^6}{(2^3 3!(4\pi)^5 v^8)}$, where we have neglected the subleading $2h$ production cross section in the large $E_{\rm cm}$ limit. By using Eq. (24), we get the scaling as $c_1\sim -0.0005\frac{ve\Delta\alpha_\mu}{m_\mu}(\frac{100v}{E_{\rm cm}})^4$, $c_0\simeq\frac{ve\Delta\alpha_\mu}{4m_\mu}$ for $E_{\rm cm}\gg 10v\sim$ TeV. This simple example also reflects why $N_{\max}\neq 1$ has a slightly smaller $\min[\sigma_{\rm tot}^{g-2}[N_{\max},E_{\rm cm}]]/\sigma_{\rm tot}^{g-2}[1,E_{\rm cm}]$ than 1. This is because, strictly speaking, the amplitude of the single Higgs production is slightly canceled by a negative and nonvanishing c_1. But we can ignore the tiny contribution when $E_{\rm cm}\gg 10v$. Since we have performed the analysis for the generic $N_{\max}$ in Fig. 4, we can conclude that the minimized inclusive cross section can be well approximated by the operator discussed in the previous section for $E_{\rm cm}=\mathcal{O}(10)$ TeV.

The multi-Higgs boson production is also a background-free process, and thus, it is easily detected. The SM background for $n>1$ might be $\mu\bar{\mu}\to\nu\bar{\nu}nh\gamma$ with $\nu\bar{\nu}$ being missed. For instance, the cross section is $\sigma_{\mu\bar{\mu}\to nh\gamma}<e^2/(16\pi^2)\times$ fb ~ 0.1 ab where we multiplied cross section

[7]Strictly speaking, the cancellation weakly depends on the $E_{\rm cm}$ via renormalization group running. Since we neglect the radiative correction to the cross section in the paper, we do not study the probe of the process by comparing the logarithmically different cross sections at different $E_{\rm cm}$. Indeed, there is an extremely unnatural scenario where the cancellation is up to $n=\mathcal{O}(100)$ so that the Higgs production with a larger n is kinetically forbidden. This scenario may only be tested by slightly changing $E_{\rm cm}$.

[8]The combination $\frac{\min\sigma_{\rm tot}^{g-2}[N_{\max},E_{\rm cm}]}{\sigma_{\rm tot}^{g-2}[1,E_{\rm cm}]}$ does not depend on $\Delta\alpha_\mu$.

of $\mu\bar{\mu} \to 2h\nu\bar{\nu}$ [45] by $e^2/16\pi^2$, which is much smaller than the signal's cross section, which is just shown to be larger than the cross section of the single Higgs production in Fig. 3. In addition, this background event should have a different feature from the signal event because the Higgs bosons, as well as the photon, are produced from the bremsstrahlung emission. They are soft. On the other hand, the Higgs bosons and the photon in the signal events are energetic. Therefore, we consider that the process is background-free. To sum up, as long as the $n = 1$ process that was discussed in the previous section can be tested, the cancellation of the amplitudes does not spoil our conclusions. This is because the cancellation scenario has a larger inclusive cross section due to $\mu\bar{\mu} \to \gamma nh$ process. This is easier to be tested by assuming a perfect detector efficiency.

So far, we have focused on the higher dimensional operators that do not include other fields than $h, \gamma, \mu, \bar{\mu}$ (and their gauge partners) and do not include derivatives to discuss the cancellation of the amplitude for $\mu\bar{\mu} \to nh\gamma$. Operators, including other SM fields, χ,[9] may contribute to the cancellation by mediating χ. We can study this case by estimating the 1PI effective action by integrating out the irrelevant fields χ. This 1PI effective action includes the terms of the form (22) in the momentum space. However, c_i are momenta-dependent functions, which may be nonlocal.[10] The relevant amplitude can be estimated by the tree-level diagrams by using the 1PI effective action. The different point is that the cancellation, in this case, is sensitive to $E_{\rm cm}$. For instance, if a $c_i \propto E_{\rm cm}^2$ term contributes to the cancellation relevant to $c_j \propto E_{\rm cm}^0$ term, the cancellation will be significantly violated if we increase $E_{\rm cm}$ by a factor of $\mathcal{O}(1)$. This is also the case by considering the diagram mediating h, γ, $\mu, \bar{\mu}$. Thus, if we change $E_{\rm cm}$ this possibility can be easily probed. Alternatively, we can also measure the anomalous reaction involving χ for testing this case.

B. HEFT without a Higgs singlet

Let us consider the so-called Higgs EFT [46–48] where the EW symmetry breaking is nonlinearly realized. In this case, the Higgs boson is a gauge singlet that may not be relevant to the chirality flip of the muon.

The muon $g-2$ operator is given as

$$f(h)\bar{\mu}_L \hat{U}_{22} F_{\mu\nu}\sigma^{\mu\nu}\mu_R; \tag{28}$$

here,

$$\hat{U} = \exp\left[i\frac{\varphi^a}{v}\sigma_a\right], \tag{29}$$

with φ^a being the electroweak (would-be) Nambu-Goldstone fields and σ_a being the Pauli matrix with $a = 1, 2, 3$. Again, $F_{\mu\nu}$ should be understood as the electromagnetic component in the electroweak gauge boson field strength. The gauge invariance is guaranteed with the gauge transformation $\hat{U} \to \hat{g}_L^{-1}\hat{U}\hat{g}_R$ and $\bar{\mu}_L \to \bar{\mu}_L\hat{g}_L, \mu_R \to \hat{g}_R^{-1}\mu_R$. $f(h)$ is a generic function for the Higgs boson, but we take $f(h) = \frac{e\Delta\alpha_\mu}{4m_\mu}$; i.e., it does not include a Higgs boson but explains the muon $g-2$. In this case, we cannot use the $h\gamma$ production to test the $g-2$. Instead, we note that

$$\hat{U}_{22} = \cos[|\varphi|/v] - i\frac{\varphi_3}{|\varphi|}\sin[|\varphi|/v], \tag{30}$$

with $|\varphi| \equiv \sqrt{\varphi_a\varphi^a}$. By using this and the equivalence theorem, there are multigauge boson production processes, e.g.,

$$\bar{\mu}\mu \to n_z Z\gamma. \tag{31}$$

The amplitude can be estimated as $|\mathcal{M}| \propto \frac{e\Delta\alpha_\mu}{4vm_\mu}|\partial_{\varphi_3}^n U_{22}|_{\varphi_a=0}| = \frac{e\Delta\alpha_\mu}{4m_\mu}\frac{1}{v^{n_z}}$. We get the cross section,

$$\sigma_Z^{g-2} \sim \left(\frac{e\Delta\alpha_\mu}{4m_\mu}\right)^2 \frac{E_{\rm cm}^{2n_z}}{(4\pi)^{2n_z-1}n_z!v^{2n_z}}. \tag{32}$$

Again, we include the phase space suppression for the order of estimate. In this case, although there is no Higgs boson production, the multigauge boson production rate is significantly increased. The cross section is shown in Fig. 5 by varying the number of the final Z bosons. One can see that energetic $E_{\rm cm} = 50$ TeV (red circle), 20 TeV (black triangle) case the cross section increases significantly with large n_z. Note that the $n_z = \mathcal{O}(10)$ background process is highly suppressed within the SM. Also, we note that $n_z \lesssim \mathcal{O}(100)$ is kinematically allowed in the $\mathcal{O}(10)$ TeV muon collider.

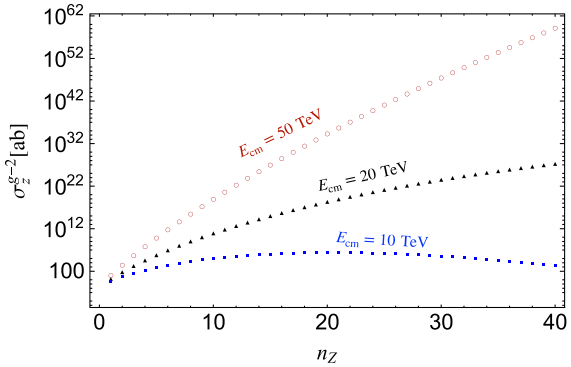

FIG. 5. $N_{\rm max}$ vs σ_Z^{g-2} for multi-Z boson production in the HEFT. The red circle (black triangle, blue square) corresponds to $E_{\rm cm} =$ 50 TeV (20 TeV, 10 TeV). We take $\Delta\alpha_\mu = 2.7 \times 10^{-9}$. The center-of-mass scale is much higher than the scale for the HEFT validity.

[9]For χ being the BSM fields, see the earlier sections.

[10]Thus, this includes the possibility that the original Lagrangian involves the derivative terms.

Such a blowup of the cross section seems to violate the perturbativity. Thus, the EFT approach may not be applicable, and we might not consider this model seriously. Here, we found that even without this prejudice, in the muon collider of $E_{\rm cm} \gtrsim 10$ TeV (blue square), this scenario can be tested by the multigauge boson productions with integrated luminosity smaller than $\mathcal{O}(1)$ fb^{-1}.

V. CONCLUSIONS

We have shown that the muon $g-2$ anomaly explanation by integrating heavy new states with a higher dimensional operator, or both can be fully tested at a muon collider with center-of-mass energy up to $\mathcal{O}(10)$ TeV and integrated luminosity of $\mathcal{O}(10)$ ab^{-1}. A model-independent approach was proposed, i.e., to produce the heaviest particle in the loop for the $g-2$ and measure its further decay into charged particles. When the heaviest particle is not reachable, we can test the lighter charged particle. If only gauge singlets are reachable, although it is not likely from the validity of the effective theory, we can measure the kinematics of its decay into the lighter charged SM particles. If the decay is to missing energy, we can measure the total number of the produced Higgs bosons, monophotons, or the cross sections of $\mu\bar{\mu} \to$ charged SM particles (see Appendix B). If all the heavy particle masses are heavier than the reach of $\mathcal{O}(10)$ TeV or there exist no heavy particles but just higher dimensional terms, we can, instead, measure $\mu\bar{\mu} \to h\gamma$, whose cross section is significantly enhanced due to the nature of the higher dimensional operator. The $\mu\bar{\mu} \to h\gamma$ process, which is the prediction of the most challenging scenario, can be tested at the 20 TeV (50 TeV) muon collider with 40 ab^{-1} integrated luminosity at the 2 $(5)\sigma$ level if the detector efficiency is perfectly good. This conclusion does not change even if the process $\mu\bar{\mu} \to h\gamma$ is unnaturally suppressed in some EFTs.

In our proposal, the QCD nonperturbative effects are no more relevant, and our theoretical estimation is not bothered by them. Even if the muon $g-2$ anomaly was due to the wrong understanding of the QCD nonperturbative effects, the muon collider can give a direction to get a deeper understanding of the nonperturbative effects. More detailed studies on collider phenomenology will be given in our future work.

ACKNOWLEDGMENTS

W. Y. would like to thank the particle and cosmology group at Tohoku University for their kind hospitality when this project was initiated. WY also thanks M. Endo, J. Hisano, T. Moroi, N. Nagata, and M. Nojiri for useful discussions. This work was supported by JSPS KAKENHI Grants No. 16H06490 (W. Y. and M. Y.), No. 19H05810 (W. Y.), No. 20H05851 (W. Y.), No. 21K20364 (W. Y.), No. 22K14029 (W. Y.), and No. 22H01215 (W. Y.).

Note added—Recently, we found Ref. [49] appeared. The authors studied the test of various higher dimensional terms, including the operator (15), at the muon collider in the context of the muon $g-2$ anomaly. Their discussions on (15) are consistent with ours. Instead of focusing on other higher dimensional operators than (15), we have proposed a generic approach to the muon $g-2$ with either renormalizable/nonrenormalizable models in the muon collider. Let us mention several relevant recent works. Importantly, Fermilab has confirmed the long-standing discrepancy of the muon $g-2$ [50]. The combined discrepancy is found to be $\Delta a_\mu = a_\mu^{\rm EXP} - a_\mu^{\rm SM} = (2.51 \pm 0.59) \times 10^{-9}$, at the 4.2σ level. There are also relevant works in the direction of the muon collider in the context of the muon $g-2$. The authors of Ref. [51] have included the strategy proposed in this work that was not included in their earlier work [21] to reach the same conclusions as us, i.e., the no-lose theorem of the muon collider. They also discussed several UV completions of the $g-2$ and their phenomena in detail, as well as the relation with fine-tuning of model parameters. Models of light singlet extension (axions, hidden photons, CP-even scalars) at the muon collider were also studied [52,53]. The authors of Ref. [54] have investigated the $\mu\bar{\mu} \to h\gamma$ in a concrete renormalizable model. The behavior when the BSM particle masses are smaller than $E_{\rm cm}$ is consistent with what we have expected in footnote 4. The process of $\mu\bar{\mu} \to h$BSMs was also studied. In most of the later studies, the estimations of $g-2$ and differential cross section, momentum distributions of the reactions, assumptions on detector efficiencies, and capability to reconstruct the Higgs decay products, and collider-specific issues are discussed precisely by assuming certain setups of a muon collider.[11] Those studies strengthen the motivation of a multi-TeV muon collider. However, the loopholes, e.g., cancellation of $\mu\bar{\mu} \to (n)h\gamma$ amplitudes with various higher dimensional terms and the $g-2$ operator in Higgsless HEFT, were not discussed in those studies. Lastly, two groups of lattice simulation have found a large discrepancy between the lattice-driven method and the R-ratio approach [56,57], confirming the result by Borsanyi *et al.* [10]. As we have mentioned, the muon collider measurement of the $g-2$, which does not suffer much from the QCD uncertainty, is then important to understand the discrepancy.

APPENDIX A: COLLIDER MEASUREMENT OF $g-2$

1. Case of BSM in reach

So far we have shown that the light particles in the $g-2$ can be tested in the muon collider diagrammatically. In our

[11] It is important to further include specific effects of a multi-TeV muon collider, such as the collinear splittings of the electroweak particles [55], in the background simulation for the BSM processes of, e.g., $\mu\bar{\mu} \to P_i^{\rm SM}\bar{P}_i^{\rm SM}$, $h\gamma$.

approach, we can measure some of the couplings in the loop.[12] This kind of measurement should be important for identifying the symmetry of the UV models. Let us assume that the BSM particle masses, charges, and spins can be measured if they are produced in the muon collider.

Here we focus on the model (9) for illustrative purposes. A more generic discussion can be possible from the diagrammatical approach by considering other possible spins and charges of the internal particles. From the detection of $\mu\bar{\mu} \to \lambda\bar{\lambda}$, we can measure the mass of λ and a combination of the coupling of λ since the production rate is proportional to $g_1^4 + g_2^4$. To measure another combination of g_1 and g_2, the production of the charged slepton is useful. Note that the angular distributions of the momenta of the outgoing particles are different between the Drell-Yan process and the bino-mediated process. For the Drell-Yan case, we obtain

$$\frac{d}{d\cos\theta}\sigma^{\text{Drell-Yan}}_{\mu\bar{\mu}\to\phi_L\phi_L^*,\phi_R\phi_R^*} \sim \frac{e^4}{32\pi E_{\text{cm}}^2}(1-\cos^2\theta). \tag{A1}$$

On the other hand, the bino-mediated one is given as

$$\frac{d}{d\cos\theta}\sigma^{g_{1,2}}_{\mu\bar{\mu}\to\phi_L\phi_L^*,\phi_R\phi_R^*} \sim \frac{g_{1,2}^4}{128\pi E_{\text{cm}}^2}\frac{1+\cos\theta}{1-\cos\theta}. \tag{A2}$$

Therefore, we expect that the new coupling $g_{1,2}$ as well as the photon coupling can be measured from the differential cross-section, e.g., forward-backward asymmetry, of the pair production for the charged sleptons. For $M_\lambda \sim m_{L,R} \gtrsim 3$ TeV, $\min[|g_1|,|g_2|] \gtrsim e$ to explain the $g-2$ by taking $\max[|g_1|,|g_2|] = \sqrt{2\pi}$. Measuring $g_{1,2}$ may be promising when the BSM particles are around or heavier than TeV.

Another possible measurement of the coupling is from the decay. If the heavier BSM particles are produced, e.g., from the right-top diagram in Fig. 1 or from the Drell-Yan process, they can decay as in the right-bottom diagram in Fig. 1. From the decay branching fraction, we can measure the coupling. For left-handed slepton there is an electroweak decay to a sneutrino and an (off shell) W boson. Since the $g-2$ loop diagram includes a "chirality" flip of the slepton and bino, the cutting-induced decay may also involve the chirality flip. By measuring the chirality of λ or μ from the production, we can have the information of δM^2 and M_λ. This decay measurement may be important in the large κ case or when the chirality allowed process is kinematically forbidden.

In addition, from $\mu\bar{\mu} \to \phi_L\phi_R^*, \phi_R\phi_L^*$, one can measure δM^2. The cross section is suppressed by $(\delta M^2/(m_L^2 - m_R^2))^2$, which leads to

$$\sigma_{\mu\bar{\mu}\to\phi_L\phi_R^*,\phi_L^*\phi_R} \sim \mathcal{O}(10)\ \text{fb}\frac{M_\lambda^2}{E_{\text{cm}}^2}\left(\frac{\delta a_\mu}{2.7\times10^{-9}}\right)^2, \tag{A3}$$

where we have assumed $|m_L - m_R| \sim m_L \sim m_R \sim M_\lambda$, $|g_1| \sim |g_2|$ and eliminated δM^2 by using Eq. (10) for illustrative purpose. Given $m_{L,R}, M_\lambda, g_{1,2}$ we see that the cross sections of the production of the opposite chirality sleptons are directly related to the value of the $g-2$. Therefore, this process is the measurement of the muon $g-2$ at the muon collider.

2. Case of BSM out of reach

Lastly let us discuss whether we can measure the $g-2$ by measuring $\mu\bar{\mu} \to h\gamma$. In general, $\mu\bar{\mu} \to h\gamma$ can happen via other higher dimension operators, which are expected in a generic model. Let us focus on other contributions from dimension 6 operators to $\mu\bar{\mu} \to h\gamma$ process with a comparable cross section. To this end, we assume that the higher dimensional operators satisfying the gauge symmetry have the similar scale $\sim M_* \equiv M/\sqrt{y_\mu} \sim 310\ \text{TeV}\frac{M}{7.6\ \text{TeV}}$. If some operator's scale is much lower than M_*, one may test those operators via other processes. We will neglect the contribution with any further suppression by y_μ, the SM particle masses, or the Higgs vacuum expectation.

Let us first consider the operators with a chirality flip of the muon. Then the operator should involve h, μ_L, μ_R, and a photon or/and derivative(s) due to the dimensionality and the gauge symmetry. One possible operator is the electric dipole moment of the muon, whose contribution in the collision does not differ from that of the $g-2$ operator. Another is the operator with derivatives,

$$\tilde{\mathcal{L}}_{\text{eff}} \sim \frac{1}{\sqrt{2}M_*^2}\partial^\nu h\overline{L_\mu}D_\nu\mu_R + \text{H.c.}, \tag{A4}$$

where we did not use covariant derivative in the Higgs boson since we concentrate on the electromagnetic part of the theory as before. By performing partial integrations and field redefinition, the resulting term is highly suppressed. We also confirmed that this term does not contribute to the $\mu\bar{\mu} \to h\gamma$ by explicitly summing all tree-level diagrams involving (A4) and renormalizable terms. Thus we do not need to consider it. The discussion also implies that $\mu\bar{\mu} \to h\gamma$ cannot be canceled by the interference of different diagrams with different dimension 6 operators with similar scales $\sim M_*$.

The discrimination of the EDM operator from the $g-2$ one, on the other hand, is more challenging in the muon collider. To measure the muon $g-2$ at the muon collider, the measurement of the muon EDM in the Fermilab [8], J-PARC [59,60], and by the proposed frozen spin experiments [61,62] are important. The future reach of the EDM operator is three orders of magnitude smaller than the corresponding muon $g-2$ discrepancy of (1).

[12]See also Ref. [58] for an approach in the ILC.

APPENDIX B: SINGLET EXTENSION OF SM EFFECTIVE THEORY

The most challenging possibility of the muon collider test of the muon $g-2$ is that there are no BSM particles in the reach of the collider, which has been discussed in Sec. III. The next to the most difficult case should be that only singlet fields are within the reach, and they only decay into weakly coupled particles, like the neutrinos or some dark sector particles. Here, we study this case.

We consider that the singlet particles, ϕs, couple to the SM sector in the effective theory with the cutoff scale M_ϕ. ϕ denotes either a boson or fermion by omitting the Lorentz index unless otherwise stated. The singlet mass scale is $m_\phi (\ll M_\phi)$. We will discuss both possibilities that the singlet couplings are renormalizable or nonrenormalizable to explain the $g-2$. We use dimensional regularization to define the loop calculation and assume that the $g-2$ contribution arises by integrating out the BSM singlet fields.

We will show that the maximal contribution to the muon $g-2$ involving higher dimensional terms are around

$$\delta a_\mu^{\mathrm{max,SESMEFT}} \equiv \frac{e m_\mu v}{16\pi^2 M_\phi^2}. \tag{B1}$$

By equating this to the observed value, we obtain $M_\phi \sim 10$ TeV. Any 1-loop contribution, $\delta a_\mu^{\mathrm{SESMEFT}}$, due to at least one higher dimensional term will be either comparable to this or further suppressed by y_μ or $1/M_\phi$. In addition, if $\delta a_\mu^{\mathrm{SESMEFT}}$ has a form of Eq. (B1) or if the singlets generate the $g-2$ via only renormalizable terms, it is fully tested in the muon collider. In other words, we will probe that any 1-loop contribution in the effective theory satisfies either $\delta a_\mu^{\mathrm{SESMEFT}} \ll \delta a_\mu^{\mathrm{max,SESMEFT}}$, i.e., the EFT is invalid, or be fully tested in the muon collider.

First of all, let us systematically study the largest 1-loop contribution to the $g-2$ operator $\bar{L}_\mu F_i^{\mu\nu} \sigma_{\mu\nu} H \mu_R$, where H is the Higgs doublet field, with F_i being the field strength for the $\mathrm{U}(1)_Y$ gauge boson ($i=Y$) or the $\mathrm{SU}(2)_L$ gauge boson ($i=2$), and L_μ being the left-handed muon doublet. Here and hereafter, we consider the symmetric phase of the electroweak gauge group, and diagonalize all the kinetic and mass terms of the relevant fields. We note from the topology that the $g-2$ Feynman diagram can only contain the vertices of the following combinations (e.g., Ref. [63]):

$$\{V_3, V_4, V_5, V_6\} = \{0,0,0,1\}, \{1,0,1,0\}, \{2,1,0,0\}, \{4,0,0,0\}, \tag{B2}$$

with V_i being the number of the i-point vertices. Those vertices must include L_μ, μ_R, γ, which could be $\mathrm{SU}(2)_L$ or $\mathrm{U}(1)_Y$ gauge boson, H and a nonzero even number of the BSM singlet field ϕ so that ϕ does not appear in the external lines.

1. {0,0,0,1} case

It is clear that the $\{0,0,0,1\}$ case requires a dimension ≥ 8 operator, which is suppressed by M_ϕ^4. The contribution is much smaller than Eq. (B1). For instance, the relevant operators include $\phi^2 H \bar{L}_\mu F_Y^{\mu\nu} \sigma_{\mu\nu} \mu_R$ with ϕ being a bosonic dimension 1 field. We can also use the $\mathrm{SU}(2)_L$ field strength as well.

2. {1,0,1,0} case

The $\{1,0,1,0\}$ case includes the diagrams of a 1PI-type and a reducible type. In the 1PI type, we need the 5-point vertex to involve a single ϕ like $\phi H \bar{L}_\mu F_Y^{\mu\nu} \sigma_{\mu\nu} \mu_R$ which is dimension 7. This is because the 3-point vertex, including ϕ, which is a singlet, cannot change the chirality of the muon. Thus the chirality should be flipped in the 5-point vertex. Therefore, the contribution is subdominant compared to Eq. (B1).

In the reducible type, the diagrams of order Eq. (B1) is a renormalization of the SM vertex, e.g., the 5-point vertex $\frac{\phi^2}{M_\phi^2} H \bar{L}_\mu \mu_R$, does not contribute to the $g-2$ since closing the loop of ϕ is the renormalization of the muon Yukawa coupling. Since we always require the IR muon mass by integrating out ϕ to be the measured one, the $g-2$ contribution is canceled. In the $\{2,1,0,0\}$ case, we have also this kind of renormalization diagram, which we will not consider.

3. {2,1,0,0} and {4,0,0,0} cases

The most nontrivial cases are $\{2,1,0,0\}$ and $\{4,0,0,0\}$. In the two cases in the broken phase, we need a 1-loop diagram with a charged internal line of SM fields and a neutral internal line involving a BSM singlet. For clarity, we separate the discussion into the three possibilities for the chirality flip for the muon.

a. Chirality flip by the SM muon Yukawa coupling

The first possibility for the chirality flip is the SM muon Yukawa interaction. In this case, the diagram should be further suppressed by y_μ. From the dimensional argument, even the largest higher dimensional contribution $\delta a_\mu^{\mathrm{SESMEFT}} = \mathcal{O}(\frac{e m_\mu^2}{16\pi^2 m_\phi M_\phi})$ is subdominant compared to Eq. (B1) by noting $M_\phi \gg m_\phi \gg v$. Strictly speaking, we also have $\delta a_\mu^{\mathrm{SESMEFT}} = \mathcal{O}(\frac{e A m_\mu^2}{16\pi^2 m_\phi^2 M_\phi})$ if ϕ is a scalar field. Since there is a dimension-1 parameter in the trilinear coupling to the Higgs fields, $A\phi|H|^2$. However, $A \lesssim m_\phi$ from the vacuum stability. This contribution is smaller.

In general, e.g., in the following subsections, we can safely neglect the superrenormalizable term. This is because this trilinear term has two Higgs fields. Then, we must further introduce a chirality flip by the SM lepton Yukawa coupling for the 1-loop contributions that are

$\propto 1/M_\phi, 1/M_\phi^2$. Therefore, we will not consider the super-renormalizable term here and hereafter.

In the case of the renormalizable interactions, the scale of the muon $g-2$ operator is controlled by m_ϕ, which is $m_\phi \sim 10^2$ GeV with $\mathcal{O}(1)$ couplings to explain the $g-2$. Since this scenario belongs to the first case of (3), we can cut the $P_i^{\rm SM}$ line to get $\mu\bar{\mu} \to P_i^{\rm SM}\bar{P}_i^{\rm SM}$ process. Here, the final states must be charged particles since the BSM particles are singlets. The cross section is no need to be chirality suppressed and is of the order,

$$\sigma_{\mu\bar{\mu}\to P_i^{\rm SM}\bar{P}_i^{\rm SM}} \sim \mathcal{O}\ ({\rm nb})\frac{m_\phi^2}{E_{\rm cm}^2}(E_{\rm cm} \gg m_\phi). \tag{B3}$$

The scaling is same as the SM background, and the size is comparable to the background. Given the large number of the events, Eq. (8), this is fully measurable and tested in the muon collider. As an example, we can consider the BSM to be a right-handed neutrino with $y_\nu H^* \phi L$. In addition, we need to have the mass term of this right-handed neutrino to preserve a lepton number symmetry to forbid a too large contribution to the active neutrino mass. The loop is closed with the photon vertex, the SM muon Yukawa vertex, and the two new vertices. This belongs to the $\{4,0,0,0\}$ case. This diagram contributes to the $g-2$ at the order $\frac{e|y_\nu|^2 m_\mu^2}{16\pi^2 m_\phi^2}$. The cross section of $\mu\bar{\mu} \to W^+_{\rm longitudinal} W^-_{\rm longitudinal}$ is of the order $\frac{|y_\nu|^2}{4\pi E_{\rm cm}^2}(E_{\rm cm} \gg m_\phi)$. Thus, they are consistent with the previous general discussion, and the model is fully tested.

b. Chirality flip by a higher dimensional term of the SM particles

The second possibility is that the chirality flip resides in the higher dimensional terms among the SM particles. As well known in the context of the SM effective theory, such a term only arises from dimension six. The largest 1-loop contribution is Eq. (B1) from the dimensional analysis.

To reach Eq. (B1), the other vertices than the dimension-6 one must be renormalizable, and the size of the couplings is $\mathcal{O}(1)$. Since, in this case, M_ϕ can be as large as $\sim$10 TeV, which is slightly below the reach of the 20 TeV muon collider, the effective theory may not be valid.

To have more robust conclusions, let us study the testability within the effective theory when $\delta a_\mu^{\rm SESMEFT} \sim \delta a_\mu^{\rm max,SESMEFT}$. We can again cut the $g-2$ loop and remove the chirality flip to obtain the scattering processes, $\mu\bar{\mu} \to P_i^{\rm SM}\bar{P}_i^{\rm SM}$, which gives a similar order of contribution as Eq. (B3). Indeed, we must have the BSM singlet couple to the muon to form a loop from the requirement of the renormalizable vertices. If the BSM singlet were not coupled to either of the external muon lines in the $g-2$ diagram, we would need ϕ-gauge boson interaction, which is not renormalizable, or ϕ-Higgs interaction, which will require an additional y_μ suppression to close the loop. Therefore, we can conclude that the muon $g-2$ is fully testable in this case with the maximized $\delta a_\mu^{\rm SESMEFT} \sim \delta a_\mu^{\rm max,SESMEFT}$.

c. Chirality flip by a term involving ϕ

The last possibility is that the chirality flip is via the vertex involving the BSM singlet. The gauge invariance implies that the singlet vertex should have dimension ≥ 5. For the dimension 6 case, the previous discussion in Appendix B 3 b applies. Namely, we can have the dominant contribution Eq. (B1), but again it is detected with the SM process. For instance, we can consider $HF_\phi^{\mu\nu}\bar{L}_\mu \sigma_{\mu\nu} l_R$ with ϕ being a gauge boson and $F_\phi^{\mu\nu}$ being the field strength or its dual, l being a SM lepton. We can have the renormalizable $\bar{\mu}_R \phi^\mu \gamma_\mu l_R$ to close the loop, which belongs to the case $\{2,1,0,0\}$. To have a large enough M_ϕ, we need $\mathcal{O}(1)$ renormalizable couplings. This is fully tested via $\bar{\mu}\mu \to \bar{l}_R l_R$ (or monophoton in the case $l_R = \mu_R$).

When the chirality-flip interaction with the BSM singlets is dimension 5, the important one is obtained from gauge invariance,

$$\frac{\phi}{M_\phi} H \bar{L}_\mu l_R. \tag{B4}$$

Here, ϕ is a BSM singlet scalar.[13] This belongs to the case of $\{2,1,0,0\}$. Our discussion here does not change by replacing L and R everywhere. We may consider closing the loop for the $g-2$ by introducing $\sim \frac{\partial_\mu \phi}{M_\phi}\bar{\mu}_R \gamma^\mu l_R$. However, by performing an equation of motion, this term becomes a similar term as (B4) with an additional suppression by a leptonic Yukawa coupling.[14] The possible chiral anomaly induced term is loop suppressed, and we can neglect it. Thus, the contribution involving the derivative coupling is subdominant.

The other possibility to close the loop without a Yukawa coupling suppression is

$$\frac{\phi}{M_\phi}(F_{\mu\nu}F^{\mu\nu} + \cdots) \quad \text{or} \quad \frac{\phi}{M_\phi}(F_{\mu\nu}\tilde{F}^{\mu\nu} + \cdots). \tag{B5}$$

Here $\cdots$ denote terms involving W, Z gauge fields for the gauge invariance. This term can be important only if

$$l = \mu. \tag{B6}$$

From a simplified Barr-Zee type loop, we obtain the contribution of the order (B1). $M_\phi \sim 10$ TeV implies that the process of

[13]The Dirac neutrino dipole moment interaction does not induce a chirality flip for a charged muon.

[14]By further introducing a Dirac neutrino Yukawa coupling of $\mathcal{O}(1)$, we cannot get the 1-loop diagram.

$$\bar{\mu}\mu \to \phi h, \qquad \bar{\mu}\mu \to \phi\gamma, \tag{B7}$$

via Eqs. (B4) and (B5) has a cross section of

$$\sigma \sim \mathcal{O}(0.1\ \text{pb}) \quad (E_{\text{cm}} \gg m_\phi), \tag{B8}$$

which is not sensitive to the energy scale. Since ϕ is assumed to decay into invisible particles, this is a mono-Higgs or monophoton process. On the other hand, the background of the SM also has a cross section of the same order at $E_{\text{cm}} = 20$ TeV [15,20]. Thus, by measuring the total number of the produced Higgs bosons/monophotons, the singlet extensions in this part are fully tested in 40 ab^{-1} muon collider.

Lastly, we comment that we may have many ϕs with a similar interaction to increase the cutoff scale M_ϕ for explaining the $g-2$ in all the previous discussions. The cross sections, discussed so far, are enhanced as well with $E_{\text{cm}} \gg m_\phi$. Therefore, our conclusions do not change.

[1] M. Davier, A. Hoecker, B. Malaescu, and Z. Zhang, Eur. Phys. J. C **77**, 827 (2017).
[2] A. Keshavarzi, D. Nomura, and T. Teubner, Phys. Rev. D **97**, 114025 (2018).
[3] G. W. Bennett *et al.* (Muon g-2 Collaboration), Phys. Rev. D **73**, 072003 (2006).
[4] B. L. Roberts, Chin. Phys. C **34**, 741 (2010).
[5] A. Keshavarzi, D. Nomura, and T. Teubner, Phys. Rev. D **101**, 014029 (2020).
[6] T. Aoyama, N. Asmussen, M. Benayoun, J. Bijnens, T. Blum, M. Bruno, I. Caprini, C. M. Carloni Calame, M. Cè, G. Colangelo *et al.*, Phys. Rep. **887**, 1 (2020).
[7] M. Lindner, M. Platscher, and F. S. Queiroz, Phys. Rep. **731**, 1 (2018).
[8] J. Grange *et al.* (Muon g-2 Collaboration), arXiv:1501.06858.
[9] T. Mibe (J-PARC g-2 Collaboration), Chin. Phys. C **34**, 745 (2010).
[10] S. Borsanyi, Z. Fodor, J. N. Guenther, C. Hoelbling, S. D. Katz, L. Lellouch, T. Lippert, K. Miura, L. Parato, K. K. Szabo *et al.*, Nature (London) **593**, 51 (2021).
[11] A. Crivellin, M. Hoferichter, C. A. Manzari, and M. Montull, Phys. Rev. Lett. **125**, 091801 (2020).
[12] A. Keshavarzi, W. J. Marciano, M. Passera, and A. Sirlin, Phys. Rev. D **102**, 033002 (2020).
[13] P. Banerjee, C. M. Carloni Calame, M. Chiesa, S. Di Vita, T. Engel, M. Fael, S. Laporta, P. Mastrolia, G. Montagna, O. Nicrosini *et al.*, Eur. Phys. J. C **80**, 591 (2020).
[14] C. M. Ankenbrandt, M. Atac, B. Autin, V. I. Balbekov, V. D. Barger, O. Benary, J. S. Berg, M. S. Berger, E. L. Black, A. Blondel *et al.*, Phys. Rev. ST Accel. Beams **2**, 081001 (1999).
[15] J. P. Delahaye, M. Diemoz, K. Long, B. Mansoulié, N. Pastrone, L. Rivkin, D. Schulte, A. Skrinsky, and A. Wulzer, arXiv:1901.06150.
[16] O. R. B. Garcia, arXiv:2009.02536.
[17] A. Costantini, F. De Lillo, F. Maltoni, L. Mantani, O. Mattelaer, R. Ruiz, and X. Zhao, J. High Energy Phys. 09 (2020) 080.
[18] M. Chiesa, F. Maltoni, L. Mantani, B. Mele, F. Piccinini, and X. Zhao, J. High Energy Phys. 09 (2020) 098.
[19] T. Han, D. Liu, I. Low, and X. Wang, Phys. Rev. D **103**, 013002 (2021).
[20] T. Han, Z. Liu, L. T. Wang, and X. Wang, Phys. Rev. D **103**, 075004 (2021).
[21] R. Capdevilla, D. Curtin, Y. Kahn, and G. Krnjaic, Phys. Rev. D **103**, 075028 (2021).
[22] S. Baek, N. G. Deshpande, X. G. He, and P. Ko, Phys. Rev. D **64**, 055006 (2001).
[23] Y. Kahn, G. Krnjaic, N. Tran, and A. Whitbeck, J. High Energy Phys. 09 (2018) 153.
[24] S. N. Gninenko and N. V. Krasnikov, Phys. Lett. B **783**, 24 (2018).
[25] P. Ballett, M. Hostert, S. Pascoli, Y. F. Perez-Gonzalez, Z. Tabrizi, and R. Zukanovich Funchal, Phys. Rev. D **100**, 055012 (2019).
[26] M. Yamaguchi and W. Yin, Prog. Theor. Exp. Phys. **2018**, 023B06 (2018).
[27] W. Yin and N. Yokozaki, Phys. Lett. B **762**, 72 (2016).
[28] T. T. Yanagida, W. Yin, and N. Yokozaki, J. High Energy Phys. 04 (2018) 012.
[29] T. T. Yanagida, W. Yin, and N. Yokozaki, J. High Energy Phys. 06 (2020) 154.
[30] M. Aaboud *et al.* (ATLAS Collaboration), J. High Energy Phys. 10 (2017) 182.
[31] A. M. Sirunyan *et al.* (CMS Collaboration), J. High Energy Phys. 06 (2018) 120.
[32] K. Abe *et al.* (Linear Collider ACFA Working Group Collaboration), arXiv:hep-ph/0109166.
[33] G. Weiglein *et al.* (LHC/LC Study Group Collaboration), Phys. Rep. **426**, 47 (2006).
[34] R. Nagai and N. Yokozaki, J. High Energy Phys. 01 (2021) 099.
[35] M. Endo and W. Yin, J. High Energy Phys. 08 (2019) 122.
[36] M. Badziak and K. Sakurai, J. High Energy Phys. 10 (2019) 024.
[37] T. T. Yanagida, W. Yin, and N. Yokozaki, J. High Energy Phys. 12 (2019) 169.
[38] T. Moroi, Phys. Rev. D **53**, 6565 (1996); **56**, 4424(E) (1997).
[39] M. Endo, K. Hamaguchi, T. Kitahara, and T. Yoshinaga, J. High Energy Phys. 11 (2013) 013.
[40] T. Behnke, J. E. Brau, P. N. Burrows, J. Fuster, M. Peskin, M. Stanitzki, Y. Sugimoto, S. Yamada, H. Yamamoto, H. Abramowicz *et al.*, arXiv:1306.6329.
[41] H. Abramowicz *et al.* (ILD Concept Group Collaboration), arXiv:2003.01116.
[42] S. Kanemura, K. Mawatari, and K. Sakurai, Phys. Rev. D **99**, 035023 (2019).

[43] Y. Aoki, K. Fujii, S. Jung, J. Lee, J. Tian, and H. Yokoya, arXiv:1902.06029.
[44] Y. Aoki, K. Fujii, S. Jung, J. Lee, J. Tian, and H. Yokoya, arXiv:2002.07164.
[45] A. Conway, H. Wenzel, R. Lipton, and E. Eichten, arXiv:1405.5910.
[46] F. Feruglio, Int. J. Mod. Phys. A **08**, 4937 (1993).
[47] C. P. Burgess, J. Matias, and M. Pospelov, Int. J. Mod. Phys. A **17**, 1841 (2002).
[48] B. Grinstein and M. Trott, Phys. Rev. D **76**, 073002 (2007).
[49] D. Buttazzo and P. Paradisi, Phys. Rev. D **104**, 075021 (2021).
[50] B. Abi *et al.* (Muon g-2 Collaboration), Phys. Rev. Lett. **126**, 141801 (2021).
[51] R. Capdevilla, D. Curtin, Y. Kahn, and G. Krnjaic, Phys. Rev. D **105**, 015028 (2022).
[52] M. Casarsa, M. Fabbrichesi, and E. Gabrielli, Phys. Rev. D **105**, 075008 (2022).
[53] R. Capdevilla, D. Curtin, Y. Kahn, and G. Krnjaic, J. High Energy Phys. 04 (2022) 129.
[54] P. Paradisi, O. Sumensari, and A. Valenti, arXiv:2203.06103.
[55] T. Han, Y. Ma, and K. Xie, J. High Energy Phys. 02 (2022) 154.
[56] M. Cè, A. Gérardin, G. von Hippel, R. J. Hudspith, S. Kuberski, H. B. Meyer, K. Miura, D. Mohler, K. Ottnad, P. Srijit *et al.*, arXiv:2206.06582.
[57] C. Alexandrou, S. Bacchio, P. Dimopoulos, J. Finkenrath, R. Frezzotti, G. Gagliardi, M. Garofalo, K. Hadjiyiannakou, B. Kostrzewa, K. Jansen *et al.*, arXiv:2206.15084.
[58] M. Endo, K. Hamaguchi, S. Iwamoto, T. Kitahara, and T. Moroi, Phys. Lett. B **728**, 274 (2014).
[59] T. P. Gorringe and D. W. Hertzog, Prog. Part. Nucl. Phys. **84**, 73 (2015).
[60] M. Abe, S. Bae, G. Beer, G. Bunce, H. Choi, S. Choi, M. Chung, W. Da Silva, S. Eidelman, M. Finger *et al.*, Prog. Theor. Exp. Phys. **2019**, 053C02 (2019).
[61] F. J. M. Farley, K. Jungmann, J. P. Miller, W. M. Morse, Y. F. Orlov, B. L. Roberts, Y. K. Semertzidis, A. Silenko, and E. J. Stephenson, Phys. Rev. Lett. **93**, 052001 (2004).
[62] A. Adelmann and K. Kirch, arXiv:hep-ex/0606034.
[63] S. Weinberg, *The Quantum Theory of Fields. Vol. 1: Foundations* (Cambridge University Press, Cambridge, England, 1995).